Quantum Frequency Translation of Single-Photon States in a Photonic Crystal Fiber

H. J. McGuinness,[1,*] M. G. Raymer,[1] C. J. McKinstrie,[2] and S. Radic[3]

[1]Oregon Center for Optics and Department of Physics, University of Oregon, Eugene, Oregon USA, 97403
[2]Bell Labs, Alcatel-Lucent, Holmdel, New Jersey 07733, USA
[3]Department of Electrical and Computer Engineering, University of California at San Diego, La Jolla, California 92093, USA

(Received 21 June 2010; published 27 August 2010; corrected 31 August 2010)

We experimentally demonstrate frequency translation of a nonclassical optical field via four-wave mixing (Bragg-scattering process) in a photonic crystal fiber (PCF). The high nonlinearity and the ability to control dispersion in PCF enable efficient translation between nearby photon channels within the visible to-near-infrared spectral range, useful in quantum networks. Heralded single photons at 683 nm were translated to 659 nm with an efficiency of 28.6 ± 2.2 percent. Second-order correlation measurements on the 683- and 659-nm fields yielded $g^{(2)}_{683}(0) = 0.21 \pm 0.02$ and $g^{(2)}_{659}(0) = 0.19 \pm 0.05$, respectively, showing the nonclassical nature of both fields.

DOI: 10.1103/PhysRevLett.105.093604 PACS numbers: 42.50.Ex, 42.50.Dv, 42.65.Ky

As more advanced quantum-information systems are created, it is likely that a quantum network will be needed [1]. A good candidate for transferring quantum information is the single photon, which is robust against loss or decoherence, and allows transfer of entanglement between remote locations. Quantum frequency translation (QFT), in which a photon at one central frequency is annihilated and another photon at a different central frequency is created [see Fig. 1(b)], serves three important purposes in quantum networks—it allows quantum devices (memories and processors) that operate at different optical frequencies to communicate via a quantum channel; it allows low-loss, long-distance exchange over fiber between two quantum devices that operate at frequencies other than the telecom ones where fiber losses are minimal; it allows photon conversion to frequencies where the optimal detectors operate. To be useful in quantum networks, QFT must (i) allow translation by any small or large photon frequency shift within the visible and near infrared to enable diverse devices to communicate, (ii) preserve the nature of the original state other than its central frequency, including any entanglement with other systems, and (iii) must be highly efficient while not introducing additional unwanted "noise" photons.

QFT using three-wave mixing in second-order $\chi^{(2)}$ nonlinear optical media can satisfy the latter two requirements. In [2] one field from a downconverted pair at 1064 nm was upconverted to green and observed to exhibit nonclassical intensity correlations with the other downconverted field. In [3] two-photon interference was observed between a 710 nm photon and one at 1550 nm, initially entangled with a 1310 nm photon. In these cases, the frequencies are far-separated. However, many other important cases exist where the two photon frequencies are nearby. For example, for constructing quantum repeaters, one needs the ability to store photons in quantum memory [4], such as an atomic Rb ensemble that absorbs and emits at wavelength 795 nm. An ideal photon source for such an experiment would be heralded maximally entangled photon-pairs, as was recently demonstrated using spontaneous parametric down-conversion at 808 nm [5]. Unfortunately, QFT using $\chi^{(2)}$ requires the difference between the two frequencies involved to equal the frequency of the strong pump field, making it prohibitive in this and many other similar cases.

In contrast, QFT using four-wave mixing (FWM) is predicted to satisfy all three above requirements [6]. It requires only that the two pump fields have a frequency difference equal to that by which one aims to translate the quantum state of interest. This, combined with flexible phase matching provided by photonic crystal fiber (PCF)

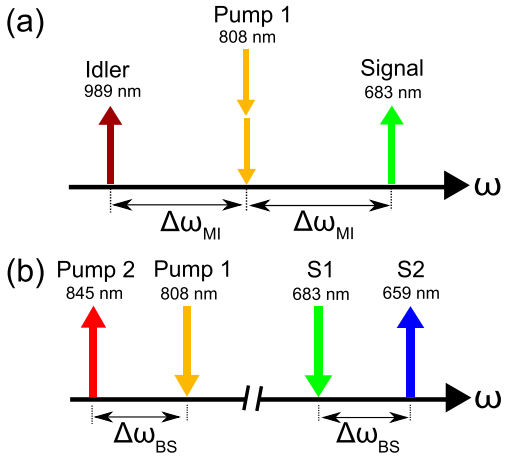

FIG. 1 (color online). (a) The modulation interaction process. Two photons from pump 1 are annihilated while two sideband photons (signal and idler), equally spaced in frequency from the pump by $\Delta\omega_{\mathrm{MI}}$, are created. Up (down) arrows indicate creation (destruction). (b) The Bragg-scattering quantum frequency translation process. Photons from pump 1 and the $S1$ mode are annihilated while photons in pump 2 and the $S2$ mode are created. The frequency separation between the pumps $\Delta\omega_{\mathrm{BS}}$ is equal to the separation $S1$ and $S2$.

as the medium, enables QFT within the visible-to-near-IR range, with no lower bound to the frequency separation of channels. We demonstrate QFT by FWM in PCF, and show that it preserves the nonclassical nature of the single-photon field being translated. We demonstrate the process, and emphasize that the FWM process in PCF allows near 100-percent efficiency between any two wavelengths in the midvisible to near IR.

The process we developed for QFT is two-pump Bragg scattering (BS), a form of nondegenerate, four-wave mixing. As opposed to other fiber-based frequency conversion processes, which involve amplification and its attendant spontaneous-emission noise, BS does not amplify the translated field, and is therefore theoretically noiseless [7]. BS is analogous to a passive beam splitter, meaning that analogues of degenerate two-photon interference apply [8]. Furthermore, it has been proved that BS is capable of translating arbitrary multiphoton states of one spectral mode to another [7]. BS was first shown classically at telecom wavelengths [9] and has been used to achieve low-noise wavelength translation from 1545 to 1365 nm with near-unity efficiency [10–12].

The $\chi^{(3)}$ BS process has additional advantages compared with sum/difference-frequency conversion in bulk and quasi-phase matched $\chi^{(2)}$ materials. Since it occurs in single-mode optical fiber, it is straightforward to couple the translated field into another fiber or other device with small loss, making it well suited for quantum networks. Also, since the efficiency is proportional to the product of the input power of each pump, one pump can be weak if the other pump compensates by being strong. PCF offers unprecedented control over the medium's dispersive properties, allowing translation to occur anywhere within the visible-to-infrared by engineering the fiber [13].

We report for the first time frequency translation in optical fiber carried out with verifiably nonclassical fields. Also, this is the first time Bragg-scattering translation in a $\chi^{(3)}$ medium has been reported in the visible regime. A single-photon wave packet with a central wavelength 683 nm is created in a PCF, shown in Fig. 2(a), and is coupled into another PCF, shown in Fig. 2(b), along with two pump fields. The BS process occurs, and with some probability (efficiency) the single-photon wave packet is translated to another wave packet with a central wavelength 659 nm (otherwise it is left alone). The translated and untranslated channels are monitored with single-photon detectors, which measure the degree of nonclassicality and the overall efficiency of the BS process.

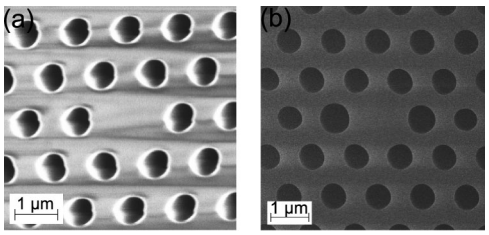

FIG. 2. (a) Scanning electron microscope (SEM) cross-sectional image of fiber 1. (b) Cross-sectional SEM image of fiber 2. The two large cladding holes near the core help to induce birefringence in the fiber.

The single-photon states that were translated were produced in a fiber via the one-pump FWM process of "modulation instability" (MI), shown in Fig. 1(a) [14,15]. In MI, two pump (P) photons are annihilated in the medium and two nondegenerate photons are spontaneously created. The central wavelengths of the produced "sideband" photons, also called signal (S) and idler (I), are determined by energy conservation ($2\omega_P = \omega_S + \omega_I$) and phase-matching requirements ($2\beta_P = \beta_S + \beta_I i$) [16]. With a single CW laser input at power P_0, fiber nonlinearity γ and fiber length L, where $P_0\gamma L \ll 1$, the state produced is given by

$$|\psi\rangle \approx |0_S, 0_I\rangle + \epsilon|1_S, 1_I\rangle + \epsilon^2|2_S, 2_I\rangle + \ldots, \quad (1)$$

where $\epsilon \ll 1$ is a function of P_0, γ and L. Since ϵ is small, the state is mostly vacuum, but if the idler (signal) channel is incident upon a detector and the detector registers an event, it is very likely that the signal (idler) is in the $|1\rangle$ Fock state. This is called heralding the signal (idler). For pulsed pump input the state is more complicated, but is not crucial for understanding the relevant physics in this Letter [17,18]. Phase matching in the PCF that we used in this experiment allows continuous tuning of the sidebands over a wide range (signal: 660–760 nm, idler: 1010–960 nm).

After single-photon wave packets are created, one is sent into a second fiber for QFT via BS [14]. Two pump fields $P1$ and $P2$ and the signal field $S1$ are coupled into the fiber, leading to the annihilation of the signal field and creation of a translated signal field $S2$, as shown in Fig. 1(b). The fields must obey energy conservation ($\omega_{P1} + \omega_{S1} = \omega_{S2} + \omega_{P2}$) and be phase matched ($\beta_{P1} + \beta_{S1} = \beta_{S2} + \beta_{P2}$) for efficient translation to occur. Treating the pumps as classical fields and the signals as quantum fields, the BS Hamiltonian is [6]

$$H = \delta(a_{S1}^\dagger a_{S1} + a_{S2}^\dagger a_{S2}) + \kappa a_{S1}^\dagger a_{S2} + \kappa^* a_{S2}^\dagger a_{S1}, \quad (2)$$

where $a^\dagger$ and a are creation and annihilation operators. The quantities δ and κ relate to the dispersion mismatch between pumps and sidebands, and the effective nonlinearity, respectively. Utilizing the spatial equations-of-motion $d_z a_j = i[a_j, H]$, the operators can be solved as functions of position along the fiber, yielding

$$a_{S1}(z) = \mu(z)a_{S1}(0) + \nu(z)a_{S2}(0), \quad (3)$$

$$a_{S2}(z) = -\nu^*(z)a_{S1}(0) + \mu^*(z)a_{S2}(0), \quad (4)$$

where the transfer functions μ and ν are

$$\mu(z) = \cos(kz) + i\delta \sin(kz)/k, \quad (5)$$

$$\nu(z) = i\kappa \sin(kz)/k, \tag{6}$$

and where $k = (|\kappa|^2 + \delta^2)^{1/2}$ and $|\mu|^2 + |\nu|^2 = 1$. The process conserves total photon number, like a beam splitter. If the parameters are set such that $|\nu(L)| = 1$, then all of the signal field will be translated to the idler field.

The above analysis is valid for single-mode, CW fields. For pulsed fields a more general theory is appropriate [8]. The temporal and spectral properties of all input fields determine the nature of the translated field. For efficient translation, temporal overlap of the fields must be maximized and care must be taken that the bandwidth of the input field is not greater than the bandwidth of the BS process, which is a function of fiber dispersion, length and pump bandwidth.

In order to demonstrate that the $S1$ input and the $S2$ output are nonclassical, the conditional second-order degree of coherence $g^{(2)}(0)$ is measured for these fields. A result of $g^{(2)}(0) < 1$ indicates a nonclassical field [19]. For a heralded field, $g^{(2)}(0)$ is given experimentally by

$$g^{(2)}(0) = \frac{N_{ABC}N_C}{N_{AC}N_{BC}}, \tag{7}$$

where A and B label the detectors monitoring the output of the heralded signal field, and C labels the heralding detector in the idler field. The quantities N_i, N_{ij}, N_{ijk} are the number of single, double coincidence, triple coincidence events between detectors i, j, and k over the time interval of the data collection, respectively [20,21].

The experimental apparatus is shown in Fig. 3. Pump 1 and pump 2 were 100 ps Ti-sapphire lasers operating at 808 and 845 nm, respectively. The lasers, having repetition rates of 76 MHz, were synchronized using a phase-locked

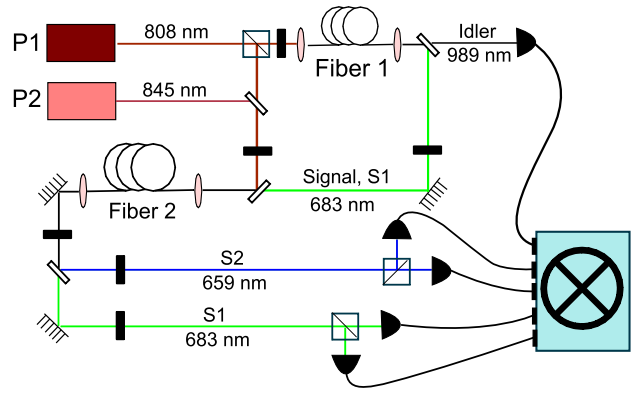

FIG. 3 (color online). Setup used to create and frequency translate single-photon states. Both pumps $P1$ and $P2$ are 100 ps Ti-sapphire lasers. A single photon is created in fiber 1 at 683-nm, heralded, and combined with $P1$ and $P2$ to be translated to 659-nm in fiber 2. Five detectors measure $g^{(2)}(0)$ of both 683- and 659-nm channels, with the 989-nm channel detector acting as the herald. Opaque rectangles represent either long-pass or bandpass filters and transparent rectangles signify dichroic mirrors.

loop, and were long-pass filtered to extinguish any light in the quantum channels. A fraction of pump 1 was sent to 32 m of a custom-made solid-core PCF, denoted as fiber 1, having a zero-dispersion wavelength (ZDW), core size and air-filling fraction of approximately 796 nm, 1.6 μm and 24%, respectively. Sidebands were created at 683 and 989 nm using MI in which phase matching was achieved using the fiber birefringence (approximately 4.3×10^{-5}) [22,23]. These beams were split, with the 989-nm idler being sent to a single-photon avalanche photodiode for heralding. Both sidebands were filtered with 13-nm bandpass filters to remove unwanted spontaneous Raman scattering.

The rest of pump 1, and all of pump 2, were combined on a dichroic mirror, with the resulting beam further combined with the 683-nm signal from fiber 1. The pulses of both pumps and the 683-nm signal pulse were overlapped temporally. All beams had the same linear polarization. All three beams were incident upon 20 meters of fiber 2 (Crystal Fibre, model number NL-PM-750, with ZDW $\sim$750 nm), and aligned on one of the principal axes of this polarization-maintaining fiber. A power of 20(30) mW from pump 1(2) was coupled into fiber 2. We achieved over 31% coupling of the 683-nm beam from fiber 1 into fiber 2 prior to translation. The state of the 683-nm field was frequency translated with a certain probability to the field centered around 659 nm. After exiting fiber 2, the pump components were filtered out of the beam, which was then separated into the 683- and 659-nm channels. Both channels were filtered with 13-nm bandpass filters. Conditional second-order correlation measurements ($g^{(2)}(0)$) of the 683- and 659-nm channels were carried out in coincidence with the 989-nm MI idler channel.

To verify that the translation process occurred with high efficiency, we measured both the depletion efficiency of the 683-nm $S1$ input and the creation efficiency of the 659-nm $S2$ output, which should be equal. The depletion efficiency was obtained by measuring the rates of counts (minus noise counts) in the output 683-nm $S1$ channel with and without the pump beams coupled into fiber 2. The depletion efficiency equals one minus the ratio of these two count rates. The result, 28.6 ± 2.2 percent, is not dependent on comparing quantum efficiencies of two detectors. To measure the creation efficiency of the 659-nm $S2$ channel, the count rate in this channel was monitored with and without the pumps. When detector efficiencies are taken into account, this measurement yields 29.4 ± 2.4 percent, agreeing with the depletion measurement to within error.

To show the nonclassical nature of the translated and untranslated light, $g^{(2)}(0)$ measurements were performed on both the 683- and 659-nm channels at the output of the fiber, yielding 0.21 ± 0.02 and 0.19 ± 0.05, respectively.

There are several factors that cause the measured values of $g^{(2)}(0)$ to be nonzero. After heralding, the photon state to

be translated is predominantly the $|1\rangle$ Fock state. But the state also includes small amplitudes for number states above 1, which increases the value of $g^{(2)}(0)$. For states generated via heralded MI there is a trade-off between higher count rates and high single-photon state probability (unless a number-resolving detector is used for heralding). Low detector efficiency (12%) for the 989-nm channel demanded higher input power than desired. Pump 1 input power in fiber 1 was chosen to give reasonably high photon flux and coincident count rates while guaranteeing the heralded state (1) was predominantly the $|1\rangle$ state. Other possible causes for increased $g^{(2)}(0)$ are accidental coincidence counts from Raman scattering, detector dark counts, and other noise. An experiment that counted N_I idler counts and N_S signal counts, both which derived from N_P pulses, would expect to register $N_I N_S/N_P$ accidental coincidences if the idler and signal beams were independent and Poisson. In our experiment the coincidence level was approximately 8.2 times higher than the expected accidental coincidence value for coincidences between the 683-nm channel and the 989-nm channel. The coincidence level for the 659-nm translated channel was approximately 6.5 times higher than the expected accidental coincidences.

These noise counts also affected the measured efficiency of the translation process. Approximately 24% of counts in the 659-nm channel, and 11% in the 683-nm channel, were from pump-induced noise, mostly from the 808-nm pump. Such noise could be greatly reduced. Because of the wavelength range of the available pumps, and the dispersion characteristics of the fibers, it was necessary for pump 1 to operate at 808 nm, which is close to fiber 2's ZDW. Operating the pump farther from the ZDW, and farther from the signal and idler modes in general, would strongly decrease the noise in these channels. Also, the Stokes and anti-Stokes Raman noise can be strongly reduced by cooling fiber 2 to liquid nitrogen temperature [24].

Theory predicts that BS is capable of 100% translation efficiency of arbitrary states [7]. In our experiment various factors limit the efficiency. The most likely factor was the relatively large spectral width of the 683-nm field created by MI. This conjecture is supported by the fact that the full width at half maximum (FWHM) of the output translated field was less than that of the input untranslated state, indicating the translation process had a narrower acceptance bandwidth than the bandwidth of the input field. These widths were measured using an input signal at 683-nm created by high-gain MI, with a FWHM of approximately 2.0 nm, while the translated field had a FWHM equal or less than 1.5 nm, the minimum width resolution of the spectrometer. The wide FWHM of the input field was due to pump 1 being close in wavelength to the ZDW of fiber 1 [18,25]. For this experiment it was unfortunately necessary for the pump and ZDW of fiber 1 to be close in wavelength, but this is not indicative of a fundamental limitation of the BS translation process.

We have demonstrated frequency translation of nonclassical states of light via the four-wave mixing Bragg-scattering process. This is the first time optical BS at the quantum level has been reported. This is also the first time translation within the visible regime has been reported. While translation in $\chi^{(3)}$ media requires two pumps, as opposed to translation in $\chi^{(2)}$ media, which requires only one, there are a number of advantages such a method offers. Because the translating device could be easily coupled to an optical fiber network, it is the clear choice for translation in a quantum network. The two-pump configuration allows for a more flexible achievement of phase-matching conditions, allowing translating between spectrally close channels. This in turn opens possibilities for two-photon (Hong-Ou-Mandel) interference between photons of different colors [8], and ultimately linear-optics quantum computing [26] using multiple frequency channels.

We thank S. van Enk for helpful comments. This work was supported by NSF Grant ECCS-0802109.

*hmcguinn@uoregon.edu

[1] J. I. Cirac *et al.*, Phys. Rev. Lett. **78**, 3221 (1997).
[2] J. M. Huang and P. Kumar, Phys. Rev. Lett. **68**, 2153 (1992).
[3] S. Tanzilli *et al.*, Nature (London) **437**, 116 (2005).
[4] M. Lobino *et al.*, Phys. Rev. Lett. **102**, 203601 (2009).
[5] S. Barz *et al.*, Nat. Photon. **4**, 553 (2010).
[6] C. J. McKinstrie *et al.*, Opt. Express **13**, 9131 (2005).
[7] C. J. McKinstrie *et al.*, Opt. Express **12**, 5037 (2004).
[8] M. G. Raymer *et al.*, Opt. Commun. **283**, 747 (2010).
[9] K. Inoue, IEEE Photonics Technol. Lett. **6**, 1451 (1994).
[10] K. Uesaka *et al.*, IEEE J. Sel. Top. Quantum Electron. **8**, 560 (2002).
[11] A. H. Gnauck *et al.*, Opt. Express **14**, 8989 (2006).
[12] D. Mechin *et al.*, Opt. Express **14**, 8995 (2006).
[13] T. A. Birks *et al.*, Opt. Lett. **22**, 961 (1997).
[14] C. J. McKinstrie *et al.*, IEEE J. Sel. Top. Quantum Electron. **8**, 538 (2002).
[15] J. Fulconis *et al.*, Opt. Express **13**, 7572 (2005).
[16] G. P. Agrawal, *Nonlinear Fiber Optics* (Academic, San Diego, 2006), 4th ed.
[17] J. Chen *et al.*, Phys. Rev. A **72**, 033801 (2005).
[18] K. Garay-Palmett *et al.*, Opt. Express **15**, 14870 (2007).
[19] R. Loudon, *The Quantum Theory of Light* (Oxford University, Oxford, 2000), 3rd ed., Chap. 5.
[20] P. Grangier *et al.*, Europhys. Lett. **1**, 173 (1986).
[21] M. Beck, J. Opt. Soc. Am. B **24**, 2972 (2007).
[22] J. Fan and A. Migdall, Opt. Express **13**, 5777 (2005).
[23] B. J. Smith *et al.*, Opt. Express **17**, 23589 (2009).
[24] H. Takesue and K. Inoue, Opt. Express **13**, 7832 (2005).
[25] M. E. Marhic *et al.*, IEEE J. Sel. Top. Quantum Electron. **10**, 1133 (2004).
[26] E. Knill *et al.*, Nature (London) **409**, 46 (2001).